Energetics of Chiral Imprinting of Cu(100) by Lysine†

Wai Yeng Cheong‡ and Andrew J. Gellman*,‡,§

Department of Chemical Engineering, Carnegie Mellon University, Pittsburgh, Pennsylvania 15213, and National Energy Technology Laboratory, Pittsburgh, Pennsylvania 15236

Received: June 15, 2010; Revised Manuscript Received: July 30, 2010

Temperature-programmed desorption experiments have been used to probe the adsorption energetics of D- and L-lysine on the chiral Cu(3,1,17)$^{R\&S}$ and achiral Cu(100) surfaces. Previous literature has reported the reconstruction of Cu(100) surfaces to form homochiral (3,1,17)^{R} facets upon adsorption of L-lysine at high coverage and after annealing to 430 K (*J. Am. Chem. Soc.* 122, **2000**, 12584). The implication of that work is that the adsorption energy of L-lysine on Cu(3,1,17)^{R} is greater than on Cu(3,1,17)^{S} and Cu(100), thereby driving the homochiral reconstruction. The results of temperature-programmed desorption measurements test and support this implication. The desorption energies of D- and L-lysine on the Cu(100) surface are significantly lower than those on either of the Cu(3,1,17)$^{R\&S}$ surfaces. Furthermore, large enantiospecific differences in desorption kinetics were observed for D- and L-lysine on the Cu(3,1,17)$^{R\&S}$ surfaces. This observed enantiospecificity is believed to originate from the enantiospecific interactions of lysine with the chiral kinked steps on these surfaces. The observation that adsorption of L-lysine on Cu(3,1,17)^{R} is energetically preferred over adsorption on Cu(3,1,17)^{S} is consistent with the formation of homochiral (3,1,17)^{R} facets during L-lysine adsorption on Cu(100).

1. Introduction

Many pharmaceuticals are chiral compounds and exist in two nonsuperimposable, mirror image forms known as enantiomers, each of which elicits different physiological effects in living systems. As a consequence, there is a significant need for enantioselective chemical processes that allow selective production of one enantiomer over the other. Many chemical processes occur on surfaces and can be made enantioselective if one uses chiral surfaces. Such chiral surfaces create a chiral environment in which the two enantiomers can be differentiated from one another. These chiral surfaces may be developed as suitable media for enantioselective separation or enantioselective heterogeneous catalysis.

One means of preparing naturally chiral surfaces is by cutting a crystal to expose a low symmetry surface with no mirror symmetry planes along its normal. Although metals do not have bulk chiral structures, they can expose chiral surfaces; typically, high Miller index planes described as having structures formed of low Miller index terraces separated by kinked step edges.[1,2] An example of this type of chiral surface is the set of naturally chiral Cu(3,1,17) surfaces shown in Figure 1. On the basis of the orientations of the microfacets that comprise the kinks, these surfaces can be denoted as Cu(3,1,17)^{S} or Cu(3,1,17)^{R}. The use of such chiral surfaces, either for enantioselective heterogeneous catalysis or for enantioselective separation, involves a fundamental elementary surface reaction step—*adsorption*. Enantiospecific adsorption is a manifestation of the difference in the interactions of the two enantiomers of a chiral compound with one enantiomer of a chiral surface. The difference in the adsorption energies of the two enantiomers on the chiral surface can be exploited to separate a racemic mixture of a chiral compound into its enantiomerically pure forms.[3]

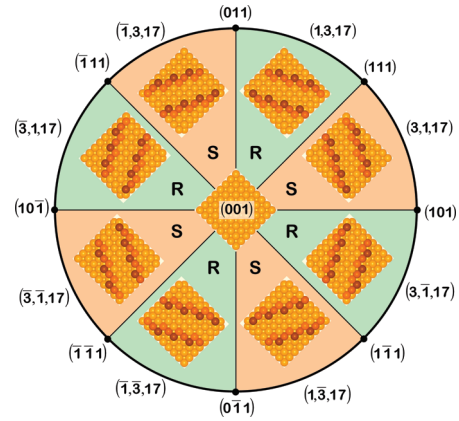

Figure 1. Stereographic projection along the (001) direction indicating the eight equivalent domains and their relative handedness. The (001) surface has a square lattice. The other domains contain illustrations of the (3,1,17) plane found in that domain. These are of alternating chirality as one goes around the (001) pole.

It was first hypothesized by McFadden et al. that high Miller index, single crystal metal surfaces which have structures characterized by kinked step edges are chiral and, therefore, should exhibit enantiospecific properties.[1] The first experimental observation that these naturally chiral metal surfaces are enantiospecific was made by Attard et al. while studying the electro-oxidation of D- and L-glucose on the Pt(643)$^{R\&S}$ surfaces.[4] They found that the Pt(643)^{S} surface exhibited a greater reactivity with L-glucose than with D-glucose. Enantiospecific adsorption and desorption of chiral adsorbates on naturally chiral surfaces was also demonstrated by Horvath et al. using temperature-programmed desorption (TPD) studies of (*R*)- and (*S*)-propylene oxide and (*R*)-3-methylcyclohexanone on the Cu(643)$^{R\&S}$ surfaces.[3,5,6] That work revealed enantiospecific differences in the adsorption energies of (*R*)- and (*S*)-propylene oxide and (*R*)-3-methylcyclohexanone on the Cu(643)$^{R\&S}$ sur-

† Part of the "Alfons Baiker Festschrift".
* Corresponding author, gellman@cmu.edu.
‡ Department of Chemical Engineering, Carnegie Mellon University.
§ National Energy Technology Laboratory.

10.1021/jp105520t
Published on Web 09/08/2010

faces. More recently, the adsorption of D- and L-cysteine on a chiral Au(17,11,9)^{S} surface was studied using X-ray photoelectron spectroscopy (XPS) and revealed enantiospecific core level binding energies in the amino and in the thiol group.[7] Held et al. reported enantiospecific adsorption of alanine on chiral Cu(531)$^{R\&S}$ surfaces using XPS, low-energy electron diffraction (LEED), and near edge X-ray absorption fine structure spectroscopy (NEXAFS).[8] There are now numerous examples of chiral probe molecules revealing enantiospecific adsorption energetics, enantiospecific surface reaction kinetics, and enantiospecific orientations when adsorbed on naturally chiral metal surfaces.

Two of the outstanding challenges in chiral surface chemistry are that of developing a predictive level understanding of the origins of enantiospecific surface chemistry and that of developing methods for the preparation of naturally chiral metal surfaces in large areas that might be amenable for application outside the laboratory. In principle, the adsorption of chiral compounds onto achiral metal surfaces can induce reconstruction to form naturally chiral planes or other naturally chiral surface features.[9] There are several studies of the adsorption of amino acids on the Cu(100) surface that reveal the formation of high Miller index Cu(3,1,17) facets as a result of amino acid adsorption and subsequent annealing.[10,11] Rankin et al. have modeled the adsorption of alanine and glycine on Cu(100) and Cu(3,1,17) and suggested that the stability of the (3,1,17) facet arises from the fact that its unit cell is quite similar in size and shape to the (4 × 2) unit cell formed by these amino acids on the Cu(100) surface.[12,13] Faceting of the Cu(100) surface can, in principle, yield the formation of eight facets in the {3,1,17} family of surfaces: four are of *S*-chirality and the other four of *R* chirality, as illustrated in Figure 1. Zhao et al. used scanning tunneling microscopy to show that annealing a high coverage of L-lysine on the achiral Cu(100) surface at 430 K for 20 min induced the formation of the four (3,1,17)^{R} facets without the appearance of any (3,1,17)^{S} facets.[10,11] Thus, L-lysine imprints its chirality onto the achiral Cu(100) surface. This phenomenon implies two things regarding the relative adsorption energies of L-lysine on Cu(100), Cu(3,1,17)^{R} and Cu(3,1,17)^{S} surfaces: $\Delta E_{ads}^{lys/(100)} < \Delta E_{ads}^{L\text{-}lys/(3,1,17)\text{-}R}$ and $\Delta E_{ads}^{L\text{-}lys/(3,1,17)\text{-}S} < \Delta E_{ads}^{L\text{-}lys/(3,1,17)\text{-}R}$ These energetic relationships define necessary conditions for chiral imprinting of achiral Cu(100) by lysine. In addition, one has the condition that the difference in surface energy between Cu(100) and Cu(3,1,17)^{R} be compensated by the difference in the L-lysine adsorption energies on these two surfaces. The enantiospecific adsorption of lysine on the Cu(3,1,17)$^{R\&S}$ surfaces and the relationships between its adsorption energetics on these and the Cu(100) surface have been studied and verified using TPD methods.

2. Experimental Section

The surface chemistry of lysine on Cu(100) and Cu(3,1,17)$^{R\&S}$ was performed in an ultrahigh vacuum (UHV) system with a base pressure of 2×10^{-10} Torr. This apparatus is equipped with an Ar^{+} ion gun for sample cleaning, a LEED optics, a mass spectrometer for TPD studies, and a homemade source for evaporative deposition of lysine vapor onto the Cu surfaces. An X-ray diffraction (XRD) system was used to determine the chirality of the Cu(3,1,17) surfaces.

All experiments other than XRD were performed in the UHV system. The Cu samples were spot-welded between two Ta wires mounted to a sample holder at the bottom of a manipulator and could be resistively heated to >1000 K and cooled to <100 K using liquid nitrogen. The sample temperature was measured with a chromel−alumel thermocouple, spot-welded to the edge of the Cu sample via a thin strip of Ni foil. The Cu samples were cleaned by repeated cycles of 1 keV Ar^{+} ion sputtering while annealing at 750 K for 500 s.

D- or L-lysine (Sigma-Aldrich, $NH_2(CH_2)_4$-CH(NH_2)-COOH, ≥98% purity) were deposited onto the Cu surface from an evaporative source consisting of a glass vial which contained either D- or L-lysine powder and was resistively heated by nichrome wire. The deposition rate was controlled by the sublimation temperature which was measured and controlled by a chromel−alumel thermocouple connected to a digital PID-temperature controller (Micromega). Exposure of the Cu sample to amino acid vapor could not be measured based on changes in background pressure of the chamber because of the very low vapor pressure of the lysine. Exposures are reported as the period of time that the Cu sample was exposed to the lysine vapor flux from the evaporative source held at 373 K. This period of exposure is controlled by a shutter placed between the evaporative source and the Cu surface. Following adsorption of D- or L-lysine at a surface temperature of 300 K, TPD measurements were performed by heating the sample at a constant heating rate (1 K/s) while the species desorbing from the surface were monitored using the mass spectrometer. The sample surface was cleaned between each TPD experiment.

3. Results

The opposing sides of the Cu(3,1,17) sample are of opposite handedness. The handedness of the Cu(3,1,17) chiral single crystal faces was identified by using XRD to determine the sense of rotation among the (111), (110), and (100) planes which intersect at the surface to form the chiral kinks. The (111), (220), and (200) reflections were used in the XRD experiments. After fixing the 2θ value calculated for each Cu(*hkl*) plane from Bragg's law, the angle, Ψ, between the (3,1,17) surface plane and the desired (*hkl*) plane was evaluated.[14] The sample was then tilted by a polar angle Ψ, followed by a 360° scan of the azimuthal angle, φ, to generate an XRD spectrum of diffraction intensity as a function of φ. The diffraction peak was located from such a φ scan after several adjustments of the polar tilt angle, Ψ, to optimize the diffraction peak intensity. The (3,1,17)^{R} and (3,1,17)^{S} surfaces are distinguished by the relative peak positions, i.e., the order of their appearance in φ. The XRD spectra obtained for the Cu(3,1,17)$^{R\&S}$ surfaces are shown in Figure 2 and reveal the chirality of the (3,1,17)^{R} and (3,1,17)^{S} surfaces. The patterns of the spacing between the diffraction peaks are clearly inverted between the two surfaces.

Adsorption of lysine on naturally chiral Cu(3,1,17)$^{R\&S}$ surfaces was studied using TPD. TPD experiments were performed following various exposures of enantiomerically pure lysine to the Cu(3,1,17)^{R} or Cu(3,1,17)^{S} surfaces. The clean Cu(3,1,17)^{R} and Cu(3,1,17)^{S} surfaces were held at 300 K and exposed to lysine vapor sublimed at 373 K. The TPD spectra recorded by monitoring the signal at $m/q = 30$ following increasing exposures of the Cu(3,1,17)^{R} surface to L-lysine are shown in the right panel of Figure 3. Two major desorption peaks were observed at approximately 360 and 470 K at the highest exposure. The peak at 360 K did not saturate with increasing exposure and, thus, is assigned to multilayer desorption. The higher temperature peak at 470 K saturated in intensity after an exposure time of ~500 s and, therefore, was attributed to desorption from the L-lysine monolayer adsorbed directly on the Cu(3,1,17)^{R} surface. The monolayer and multilayer desorption peaks were found to have similar fragmentation patterns (Table 1) which match the fragmentation pattern of lysine,

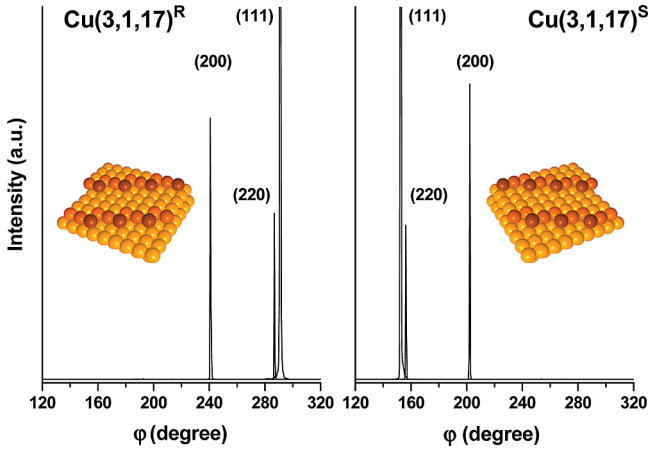

Figure 2. XRD scans obtained for $Cu(3,1,17)^R$ and $Cu(3,1,17)^S$ as functions of azimuthal angle, φ, at polar angles, Ψ, containing the (200), (220), and (111) reflections. The relative ordering of the diffraction peaks indicate the handedness of the Cu(3,1,17) substrate. The absolute azimuthal angles are arbitrary because the starting position for the φ scan is arbitrary.

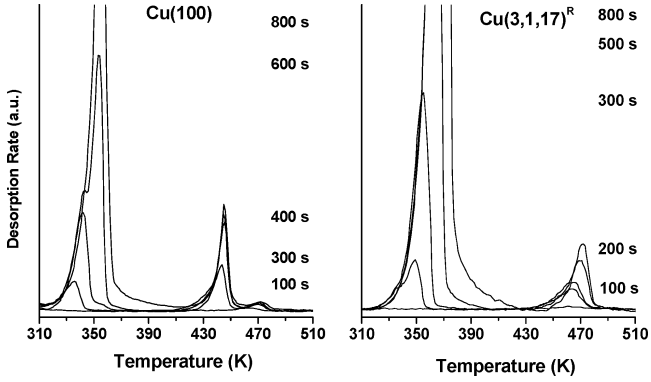

Figure 3. TPD spectra of L-lysine from chiral and achiral copper surfaces. The left-hand panel shows desorption of L-lysine from the Cu(100) surface for exposure times of 100, 300, 400, 600, and 800 s. Two major desorption peaks are visible at the highest exposure: monolayer desorption at ~445 K and multilayer desorption at ~360 K. The high-temperature tail at ~470 K may arise from desorption from step edges and matches such features observed on Cu(3,1,17). The right-hand panel shows desorption of L-lysine from the $Cu(3,1,17)^R$ surface for exposure times of 100, 200, 300, 500, and 800 s. Monolayer desorption occurs at ~470 K, i.e., ~25 K higher than that on the Cu(100) surface. TPD spectra were collected by monitoring the signal at $m/q = 30$ while heating the surface at 1 K/s.

TABLE 1: Fragmentation Patterns for L-Lysine Desorbing from Cu(3,1,17) and Cu(100)

	Cu(100)		$Cu(3,1,17)^R$	
	multilayer	monolayer	multilayer	monolayer
m/q	360 K	445 K	360 K	470 K
28	61	63	53	50
30	100	100	100	100
44	63	70	56	60
52	6.9	7.9		
56	55	54		
67	4.5	3.8		
84	16	16		

indicating that both peaks arise from desorption of intact lysine molecules. The monolayer and multilayer peaks grew almost simultaneously before the saturation of the first layer, suggesting that lysine molecules adsorb into second and subsequent layers before completely filling the first layer. This layer growth mechanism on metal surfaces is common for other amino acids.[15–17] Heating the $Cu(3,1,17)^R$ surface during TPD experiments resulted in thermal decomposition of some L-lysine molecules in the first layer, as revealed by the complex behavior of signals for various m/q ratios at temperatures above the monolayer desorption temperature of 470 K (data not shown). The TPD spectra acquired under the same conditions for L-lysine on the $Cu(3,1,17)^S$ surface, for D-lysine on the $Cu(3,1,17)^R$ surface, and for D-lysine on the $Cu(3,1,17)^S$ surface were all qualitatively similar to those shown in the right panel of Figure 3.

TPD may be used to detect desorption from different adsorption sites on a surface.[3] As depicted in Figure 2, the $Cu(3,1,17)^{R\&S}$ surfaces consist of narrow (100) terraces separated by monatomic steps with kink sites along the step edge. Nevertheless, there is only one peak associated with lysine desorption from the monolayer adsorbed directly on the $Cu(3,1,17)^{R\&S}$ surfaces. In our attempt to assign this single monolayer desorption feature to a specific adsorption site on the Cu(3,1,17) surface, comparison was made with lysine desorption from the Cu(100) surface (left panel of Figure 3). Desorption of lysine in the monolayer on the Cu(100) surface occurs at 445 K while the multilayer desorption feature occurs at ~360 K, as on $Cu(3,1,17)^R$. Comparison of the mass spectral fragmentation pattern (Table 1) for the lysine desorption feature at 445 K and that of the multilayer suggests that the feature at 445 K arises from desorption of intact L-lysine. If L-lysine molecules are desorbing from the (100) terraces of the $Cu(3,1,17)^R$ surface, the TPD features should be similar to those observed from the Cu(100) surface. Instead, the saturated L-lysine monolayer desorbed from the $Cu(3,1,17)^R$ surface at ~25 K higher than from the Cu(100) surface. A closer view of the first-layer peak on Cu(100) reveals a high-temperature tail which saturates in intensity at relatively low initial coverage and does not increase in size proportional to the first-layer peak. This high-temperature tail may arise from desorption of L-lysine from step defects on the Cu(100) surface. In fact, the desorption temperature of this feature, ~470 K, is identical to that of the L-lysine monolayer from the $Cu(3,1,17)^R$ surface. Therefore, it is likely that the desorption peak of the L-lysine monolayer on the $Cu(3,1,17)^R$ surface corresponds to lysine desorption from the kinked steps on the surface. The single desorption peak from the L-lysine monolayer on Cu(3,1,17) suggests that there is no room for the adsorption of two lysine molecules per unit cell on an ideal Cu(3,1,17) surface. This means that the structure of the Cu(3,1,17) surface does not have sufficient area per unit cell to accommodate adsorption of large molecules, such as lysine, at both the step edge and on the terrace. While, in reality, the roughened surface has regions with wider terraces than those observed for the ideally terminated surface, the added terrace area does not seem to allow adsorption of lysine on both step edges and terraces.[18] Because adsorption sites at the kinked step allow an adsorbed molecule to interact with more Cu atoms than adsorption on the flat terrace, the adsorption energies and hence, the desorption temperature of lysine adsorbed at a step edge should be higher than that of molecules adsorbed on the (100) terrace. Comparison of the TPD spectra shown in Figure 3 of L-lysine on Cu(3,1,17) and on Cu(100) supports this statement.

If adsorption of L-lysine on the kinked steps of $Cu(3,1,17)^{R\&S}$ surfaces is enantiospecific, desorption of the L-lysine monolayer from $Cu(3,1,17)^R$ and $Cu(3,1,17)^S$ ought to reveal a difference in peak desorption temperatures. TPD experiments were performed after allowing $Cu(3,1,17)^R$ or $Cu(3,1,17)^S$ to be saturated by L-lysine by exposing the surface to L-lysine vapor for 800 s. Figure 4 shows the TPD spectra recorded for saturation

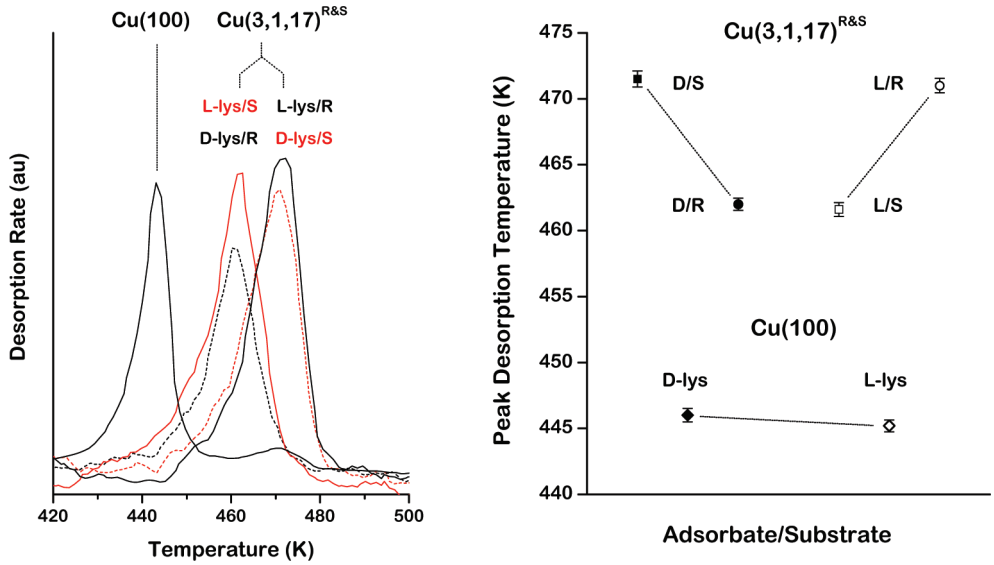

Figure 4. Left-hand panel. TPD of L-lysine from the $Cu(3,1,17)^{R\&S}$ surfaces following exposure to L-lysine for 800 s. The highest temperature desorption features from the $Cu(3,1,17)^{R\&S}$ surfaces reveals a difference in peak desorption temperatures of 9.5 ± 0.8 K. TPD spectra were collected at a heating rate of 1 K/s while monitoring the signal at $m/q = 30$. Right-hand panel. Plot of peak desorption temperatures of L-lysine and D-lysine on the $Cu(3,1,17)^{R}$, $Cu(3,1,17)^{S}$, and Cu(100) surfaces. Error bars correspond to 1 standard deviation in the temperature measurements and have been determined from six repetitions of each TPD spectrum. The results on the $Cu(3,1,17)^{R}$ and $Cu(3,1,17)^{S}$ surfaces reveal a clear and significant diastereomeric effect.

coverages of L-lysine on the $Cu(3,1,17)^{R}$ and $Cu(3,1,17)^{S}$ surfaces. The TPD spectra reveal a clear difference between the monolayer peak desorption temperatures on the $Cu(3,1,17)^{R}$ and $Cu(3,1,17)^{S}$ surfaces. These measurements were repeated six times to obtain a meaningful measure of the peak temperature differences. The peak maxima were fit with Gaussian curves using data from a temperature range of ±8 K about each monolayer peak, and the peak temperature was determined from the maximum in the Gaussian fit. L-Lysine desorbs from the $Cu(3,1,17)^{R}$ surface at a temperature 9.4 ± 0.8 K higher than that from the $Cu(3,1,17)^{S}$ surface, indicating that L-lysine has a higher adsorption energy on the $Cu(3,1,17)^{R}$ surface than on the $Cu(3,1,17)^{S}$ surface. To demonstrate that this is truly the result of enantiospecificity, it is necessary to show that the desorption temperature for D-lysine on the $Cu(3,1,17)^{R\&S}$ surfaces differs by an amount that is equal but opposite to that of L-lysine on these surfaces. The TPD spectra for the D-lysine monolayer are also shown in the left-hand panel of Figure 4. D-Lysine desorbs from the $Cu(3,1,17)^{R}$ surface at a temperature 9.5 ± 0.8 K lower than from the $Cu(3,1,17)^{S}$ surface, indicating that D-lysine has a lower adsorption energy on the $Cu(3,1,17)^{R}$ surface than on the $Cu(3,1,17)^{S}$ surface. As a final control one can compare the desorption temperatures of D- and L-lysine monolayers on the Cu(100) surfaces. They differ by 0.8 ± 0.8 K. The diastereomeric relationship between the desorption spectra and the peak desorption temperatures is illustrated in the two panels of Figure 4 and indicates that the enantiospecificity of the adsorption of D- and L-lysine with the $Cu(3,1,17)^{R\&S}$ surfaces is real and significant.

4. Discussion

The desorption kinetics of D- and L-lysine are clearly enantiospecific as established by the diastereomeric relationship in the peak desorption temperatures measured during TPD experiments and illustrated in Figure 4. It is worth noting that the enantiospecificity of these desorption temperatures and corresponding adsorption energies is quite high relative to most prior observations of enantioselectivity on naturally chiral metal surfaces. In similar experiments with (*R*)-3-methylcyclohexanone adsorbed on various chiral Cu surfaces, the greatest enantiospecific difference in desorption temperature that we have observed is ~4 K.[3,5,19] The enantiospecific difference in peak desorption temperatures for D- and L-lysine on $Cu(3,1,17)^{R\&S}$ surfaces is $\Delta T_p = 9.5 \pm 0.8$ K. The only greater such enantiospecific difference in molecular desorption temperatures, of which we are aware, is $\Delta T_p = 15$ K observed for methyl lactate on the $Cu(643)^{R}$ surface.[20]

The peak desorption temperatures in TPD spectra are reflective of adsorption energetics. To a first approximation, the enantiospecific difference in adsorption energies, $\Delta\Delta E_{ads}$, can be determined by the corresponding enantiospecific difference in peak desorption temperatures (ΔT_p) using the Redhead relation.[21] This has been done assuming a first-order form for the desorption process and a pre-exponential factor of $\nu = 10^{13}$ s^{-1}. For chiral lysine on the $Cu(3,1,17)^{R\&S}$ surfaces, the enantiospecific difference in adsorption energies is $\Delta\Delta E_{ads} = 2.6 \pm 0.3$ kJ·mol^{-1}. This difference is the fundamental basis for enantioselective discrimination of chiral compounds. The TPD spectra also indicate that the adsorption energy of lysine on the Cu(3,1,17) surfaces is greater than that on the Cu(100) surfaces. In particular, the adsorption energy of L-lysine on $Cu(3,1,17)^{R}$ (or D-lysine on $Cu(3,1,17)^{S}$) is greater than that on Cu(100) by $\Delta\Delta E_{ads} = 6.7 \pm 0.3$ kJ·mol^{-1}.

It is important to note, that the energetics determined for desorption of L-lysine from Cu surfaces may not correspond directly to adsorption energies. In fact, it is surprising that lysine desorbs from the monolayer as an intact molecule. Amino acids adsorb on Cu via deprotonation of the carboxylic acid group.[12,13] Glycine and alanine on Cu(110) are adsorbed in the deprotonated form and during TPD experiments decompose at temperatures of ~450 K.[8,22,23] We have also observed decomposition of alanine on Cu(110). The fragmentation patterns listed in Table 1 suggest that lysine differs from alanine in the sense that some fraction of the monolayer desorbs intact at ~450 K. This must occur by a recombinative process with hydrogen atoms; however, hydrogen desorption from Cu occurs at much lower

temperatures and so, it is not clear what the source of hydrogen is. One apparent difference between alanine and lysine is that prior studies of lysine on Cu(110) suggest that it adsorbs as a zwitterion, $NH_2(CH_2)_4-CH(NH_3)-COO$, by transfer of the proton from the carboxyl group to the α-amine.[24,25] This has not been suggested for alanine which is believed to be adsorbed in the deprotonated form, $CH_3-CH(NH_2)-COO$. Perhaps the molecular desorption of lysine at 450 K arises from intermolecular proton transfer followed by desorption. This is actually a recombinative process, and thus, the energetics measured from TPD experiments correspond to the barriers to recombinative desorption. These differ from the desorption energies by amounts corresponding to the barriers to dissociative adsorption of the lysine. Thus, our estimate of the enantiospecific difference in adsorption energies, $\Delta\Delta E_{ads} = 2.6 \pm 0.3$ kJ·mol^{-1}, assumes that the barriers to dissociative adsorption of lysine are not enantiospecific.

Most importantly, the results presented here are directly relevant to the understanding of chiral imprinting of surfaces by molecular adsorption. They demonstrate a system in which the energetic constraints are such that adsorption of a chiral molecule onto an achiral substrate will drive homochiral faceting. Prior work by Zhao et al.[11] reported the homochiral faceting of Cu(100) by adsorption of L-lysine to form intrinsically chiral $(3,1,17)^R$ facets with the absence of $(3,1,17)^S$ facets. We have demonstrated that the adsorption energy of L-lysine on the $Cu(3,1,17)^{R\&S}$ surface is higher than that on the Cu(100) surface by $\Delta\Delta E_{ads} = 6.7 \pm 0.3$ kJ·mol^{-1}, providing the energetic driving force for the formation of (3,1,17) facets upon adsorption of high coverage lysine on Cu(100) under suitable conditions. Furthermore, our finding that L-lysine energetically prefers adsorption on $Cu(3,1,17)^R$ over adsorption on $Cu(3,1,17)^S$ by $\Delta\Delta E_{ads} = 2.6 \pm 0.3$ kJ·mol^{-1} is consistent with the observed homochiral formation of $(3,1,17)^R$ facets. All of these results are consistent with the reports of Zhao et al. of the homochiral faceting of Cu(100) during adsorption of L-lysine.[10,11] More importantly, they illustrate the conditions necessary for the general phenomenon of chiral imprinting of achiral surfaces by adsorption of chiral compounds. Finally, the desorption feature at 470 K in the TPD spectra from the Cu(100) surface (Figures 3 and 4) is consistent with the desorption of L-lysine from R-kinks rather than S-kinks, indicating chiral imprinting.

5. Conclusions

Adsorption of chiral lysine was found to exhibit significant enantiospecificity on the $Cu(3,1,17)^{R\&S}$ surfaces. This system also allowed the observation of true diastereomerism effect in the molecular desorption of a chiral molecule from naturally chiral single crystal surfaces. L-Lysine was found to have a higher adsorption energy on the $Cu(3,1,17)^R$ surface than on the $Cu(3,1,17)^S$ surface, while D-lysine was found to have a higher adsorption energy on the $Cu(3,1,17)^S$ surface than on the $Cu(3,1,17)^R$ surface. The observed enantiospecificity is believed to come from the enantiospecific interactions of lysine with the chiral kinked steps on the surface. The results presented here corroborated the previous finding that adsorption of L-lysine on Cu(100) can induce reconstruction of the underlying substrate to form (3,1,17) facets due to the difference in adsorption energies of lysine on Cu(3,1,17) and on Cu(100).[11] These facets appeared only with *R*-chirality due to the enantiospecific preference in adsorption energies for L-lysine adsorption on $(3,1,17)^R$ rather than $(3,1,17)^S$ surfaces.

Acknowledgment. This work has been supported by Department of Energy under Grant No. DE-SC0002448.

References and Notes

(1) McFadden, C. F.; Cremer, P. S.; Gellman, A. J. *Langmuir* **1996**, *12*, 2483–2487.
(2) Sholl, D. S.; Asthagiri, A.; Power, T. D. *J. Phys. Chem. B* **2001**, *105* (21), 4771–4782.
(3) Horvath, J. D.; Koritnik, A.; Kamakoti, P.; Sholl, D.; Gellman, A. J. *J. Am. Chem. Soc.* **2004**, *126*, 14988–14994.
(4) Ahmadi, A.; Attard, G.; Feliu, J.; Rodes, A. *Langmuir* **1999**, *15* (7), 2420–2424.
(5) Horvath, J. D.; Gellman, A. J. *J. Am. Chem. Soc.* **2002**, *124*, 2384–2392.
(6) Horvath, J. D.; Gellman, A. J. *J. Am. Chem. Soc.* **2001**, *123*, 7953–7954.
(7) Schillinger, R.; Sljivancanin, Z.; Hammer, B.; Greber, T. *Phys. Rev. Lett.* **2007**, *98*, 136102(1)–136102(4).
(8) Gladys, M. J.; Stevens, A. V.; Scott, N. R.; Jones, G.; Batchelor, D.; Held, G. *J. Phys. Chem. C* **2007**, *111* (23), 8331–8336.
(9) Chen, Q.; Richardson, N. V. *Prog. Surf. Sci.* **2003**, *73* (4−8), 59–77.
(10) Zhao, X.; Zhao, R. G.; Yang, W. S. *Langmuir* **2000**, *16*, 9812–9818.
(11) Zhao, X. *J. Am. Chem. Soc.* **2000**, *122*, 12584–12585.
(12) Rankin, R. B.; Sholl, D. S. *Surf. Sci.* **2005**, *574*, L1–L8.
(13) Rankin, R. B.; Sholl, D. S. *J. Phys. Chem. B* **2005**, *109*, 16764–16773.
(14) Kittel, C. *Introduction to solid state physics*, 7th ed.; John Wiley & Sons, Inc.: New York, 1995.
(15) Gao, F.; Li, Z.; Wang, Y.; Burkholder, L.; Tysoe, W. T. *J. Phys. Chem. C* **2007**, *111*, 9981–9991.
(16) Gao, F.; Li, Z.; Wang, Y.; Burkholder, L.; Tysoe, W. T. *Surf. Sci.* **2007**, *601*, 3276–3288.
(17) Gao, F.; Wang, Y.; Burkholder, L.; Tysoe, W. T. *Surf. Sci.* **2007**, *601*, 3579–3588.
(18) Baber, A. E.; Gellman, A. J.; Sholl, D. S.; Sykes, E. C. H. *J. Phys. Chem. C* **2008**, *112* (30), 11086–11089.
(19) Horvath, J. D.; Gellman, A. J. *Top. Catal.* **2003**, *25*, 9–15.
(20) Fleming, C.; King, M.; Kadodwala, M. *J. Phys. Chem. C* **2008**, *112* (47), 18299–18302.
(21) Redhead, P. A. *Vacuum* **1962**, *12*, 203–211.
(22) Jones, G.; Jones, L. B.; Thibault-Starzyk, F.; Seddon, E. A.; Raval, R.; Jenkins, S. J.; Held, G. *Surf. Sci.* **2006**, *600*, 1924–1935.
(23) Barlow, S. M.; Raval, R. *Surf. Sci. Rep.* **2003**, *50* (6−8), 201–341.
(24) Humblot, V.; Methivier, C.; Pradier, C. M. *Langmuir* **2006**, *22*, 3089–3096.
(25) Tielens, F.; Humblot, V.; Pradier, C. M. *Surf. Sci.* **2008**, *602* (5), 1032–1039.

JP105520T